

Structural and electronic properties of Bi_2Se_3 topological insulator thin films grown by Pulsed Laser Deposition

P.Orgiani,^{1,2,a)} C.Bigi,^{2,3} P.Kumar Das,² J.Fujii,² R.Ciancio,² B.Gobaut,⁴ A.Galdi,^{1,5} C.Sacco,^{1,6} L.Maritato,^{1,6} P.Torelli,² G.Panaccione,² I.Vobornik,² and G.Rossi^{2,3}

¹⁾ *CNR-SPIN, UOS Salerno, 84084 Fisciano, Italy.*

²⁾ *CNR-IOM, TASC Laboratory, 34139 Trieste, Italy.*

³⁾ *Department of Physics, University of Milano, 20133 Milano, Italy.*

⁴⁾ *Elettra Sincrotrone Trieste, 34139 Trieste, Italy.*

⁵⁾ *Department of Information and Electrical Engineering and Applied Mathematics, University of Salerno, 84084 Fisciano, Italy.*

⁶⁾ *Department of Industrial Engineering, University of Salerno, 84084 Fisciano, Italy.*

(Dated: April 12, 2017)

We report on epitaxial growth of Bi_2Se_3 topological insulator thin films by Pulsed Laser Deposition (PLD). X-ray diffraction investigation confirms that Bi_2Se_3 with single (001)-orientation can be obtained on several substrates in a narrow (i.e. 20°C) range of deposition temperatures and at high deposition pressure (i.e. 0.1 mbar). However, only films grown on (001)- Al_2O_3 substrates show an almost-unique in-plane orientation. In-situ spin-resolved ARPES experiments, performed at NFFA-APE facility of IOM-CNR and Elettra (Trieste), show a single Dirac cone with the Dirac point at $E_B \sim 0.38\text{ eV}$ located in the center of the Brillouin zone and the spin polarization of the topological surface states. These results demonstrate that topological surface state can be obtained in PLD-grown Bi_2Se_3 thin films.

I. INTRODUCTION

Over the last decade, topological insulators have attracted great interest for their intriguing conduction mechanisms^{1–3}. Even though they are insulating in the bulk, they show a metallic surface state characterized by a unique spin texture, as unambiguously demonstrated by spin-resolved ARPES experiments^{4–7}. Furthermore, these states are topologically protected against scattering driven by strong spin-orbit interaction thus being attractive as functional materials for spintronics applications^{8,9}. However, for both fundamental studies as well as electronic applications, high-quality single-crystalline Bi_2Se_3 thin films, exhibiting topologically protected surface states, are therefore necessary. Moreover, since most of the electronic devices are based on ad-hoc tailored multi-layered heterostructures, it is equally necessary to use flexible thin film deposition techniques which would allow the growth of a large variety of functional materials within the same growth system.

In a Pulsed Laser Deposition (PLD) system, the single-atomic species of complex materials are supplied through an ablation process of a target in form of polycrystalline powders and/or single crystal by the irradiation of a high-intense laser beam. Therefore, multi-layered heterostructures can be easily engineered by positioning the different targets along the laser path, in a continuous vacuum condition. PLD shares with other deposition techniques, such as Molecular Beam Epitaxy (MBE), the high cleanliness of the system to prevent any possible contamination and the extremely low deposition rate achievable during

the growth (down to 0.01 nm/s). Moreover, since the propagation of the ablated plume of materials is stopped only at very high pressure (i.e. several mbar), deposition processes at such high partial pressures are indeed possible. Such a capability is particularly important during the growth of materials containing highly volatile atoms (e.g. selenium in the present case), whose re-evaporation rate can be reduced by increasing the background pressure.

We here report on the growth at very high Ar pressure (i.e. 0.1 mbar) of Bi_2Se_3 thin films. Combining low deposition temperatures ($\sim 290^\circ\text{C}$) and low deposition rate is the recipe to epitaxially grow Bi_2Se_3 . We show that the template substrate, while not influencing the bulk structural properties, does have a tremendous impact on the surface structural properties of the films. Highly-textured single domain (001)-oriented Bi_2Se_3 can only be grown on (001) Al_2O_3 substrates. Our in-situ synchrotron radiation x-ray photoemission spectroscopy (XPS), angular resolved photoemission spectroscopy (ARPES) and spin-resolved ARPES data and ex-situ X-ray diffraction (XRD) data prove that we succeeded in growing by PLD high quality Bi_2Se_3 thin films whose surface hosts the topologically protected surface state with expected helical spin texture.

Bi_2Se_3 thin films were grown by PLD technique, at the NFFA-APE facility of IOM-CNR and Elettra in Trieste¹⁰, using a KrF excimer pulsed laser source ($\lambda = 248\text{ nm}$), with a typical energy density of about 2 J/cm^2 , under a ultra-pure (99.9999%) Ar pressure. Laser pulses were focused on a stoichiometric polycrystalline Bi_2Se_3 target (purity 99.999%). The typical deposition rate was about 0.07 nm per laser shot and the laser repetition rate was varied from 1 to 10 Hz. Struc-

^{a)} Electronic mail: pasquale.orgiani@spin.cnr.it

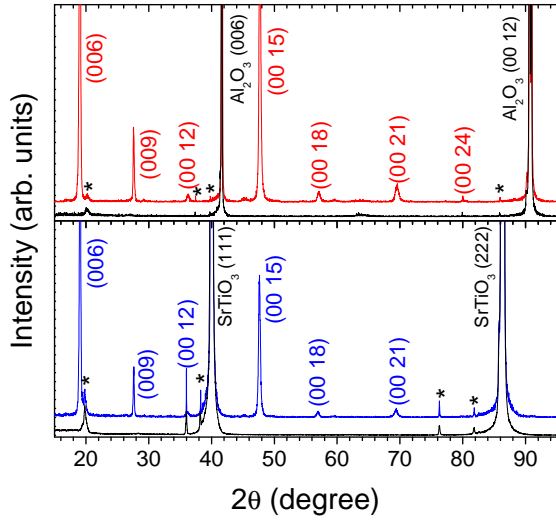


Figure 1. Symmetrical $\theta - 2\theta$ scan of a Bi_2Se_3 thin film grown on a (001)- Al_2O_3 (red curve in upper panel) and SrTiO_3 (blue curve in lower panel) substrates. For reference, the spectra of bare (001)- Al_2O_3 and (111)- SrTiO_3 substrates are also reported as black curves (asterisks indicate spurious peaks recorded by diffractometer on both films and bare substrates).

tural properties of thin films were characterized by in-situ Low-Energy Electron Diffraction (LEED) and ex-situ XRD, using a four-circles diffractometer with a $\text{Cu K}\alpha$ radiation source. XPS and ARPES measurements were performed at the APE-NFFA beamline end stations receiving undulator synchrotron radiation from the Elettra storage ring in UHV spectrometer chambers directly connected with the in-situ PLD growth apparatus thus allowing the in-situ transferring of the samples.

Bi_2Se_3 shows a rhombohedral crystal structure (space group $R\bar{3}m:H$) with a periodic stacking of Bi-Se quintuple layers along the out-of-plane c -axis. The unit cell spans three Bi-Se quintuple layers with lattice constants along a -axis and c -axis of 0.414 nm and 2.864 nm, respectively^{11,12}. Remarkably, even though most of the substrates used for the growth have very different in-plane lattice parameters (e.g. (001) Al_2O_3 ¹³, (111) SrTiO_3 ¹⁴, (001) Si¹⁵, (111) Si^{16,17}, (111) InP¹⁸), highly c -axis oriented Bi_2Se_3 thin films have been deposited in all of the cases. However, azimuthal ϕ -scans typically show a six-fold symmetry rather than the expected three-fold one, thus indicating that the film in-plane texturing derives from two domains, 60° rotated with respect to each other^{13,18,19}. We here show that such a two-domain in-plane texturing can be substantially removed by using a suitable substrate.

Bi_2Se_3 thin films were deposited on both (001) Al_2O_3 and (111) SrTiO_3 single crystals. The temperature of the substrate ranged from 270°C up to 400°C . After the film growth, the samples were cooled down to room temperature in about 30 minutes in argon at deposition pressure ranging from 10^{-5} up to 10^{-1} mbar. Growth process at low Ar pressure (i.e. below 10^{-1} mbar) was found

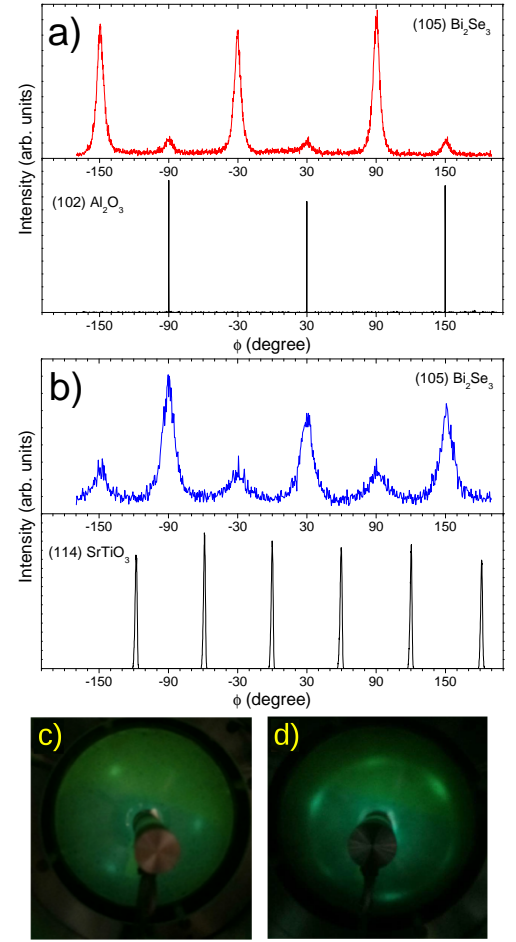


Figure 2. Azimuthal ϕ -scans around the (105) Bi_2Se_3 asymmetric reflections for Bi_2Se_3 films grown on Al_2O_3 (panel a) and SrTiO_3 (panel b) substrates, respectively; as reference, azimuthal ϕ -scans around the (102) Al_2O_3 and the (114) SrTiO_3 asymmetric reflections are also reported as black curves in the panels; c-d) LEED patterns of Bi_2Se_3 thin films grown on Al_2O_3 and SrTiO_3 substrates, respectively.

to promote Bi segregation, as measured by XPS on the Bi-4f and Se-3d core levels. Similarly, by increasing the growth temperature, Se deficiency is promoted until the Bi_3Se_4 phase stabilizes for a growth temperature of about 330°C . Such a result is not surprising since the Bi_3Se_4 shares with the Bi_2Se_3 the same rhombohedral crystal structure, with a slightly larger cell length a of 0.422 nm. However, due to the sizable difference in the c -axis lattice parameter (i.e. 4.04 nm), the two phases can be discriminated by XRD. A further increase of the temperature turns the film into an amorphous alloy and no diffraction peaks were measured. Best results were obtained for a growth temperature of 290°C and low repetition rate of laser pulses (i.e. 1 Hz), under an Ar pressure of 10^{-1} mbar. Interestingly, at such a high deposition pressure, the target-to-substrate distance was crucial in getting the optimal Se:Bi chemical ratio. The optimal target-to-substrate distance, in our geometry, was found

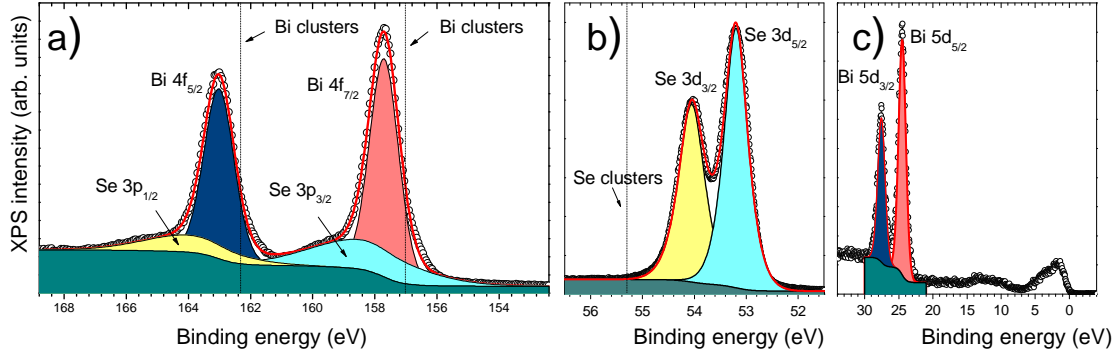


Figure 3. High-resolution XPS scans of Se-3p/Bi-4f peaks (panel a), Se-3d peaks (panel b) and Bi-5d peaks along with the valence band (panel c); excitation photon energy is 920 eV. Results of fitting procedures are also reported; expected binding energies for both Bi and Se segregation are also reported in panel a) and b), respectively.

to be 48 nm. As a matter of fact, like other complex system²⁰, as the background pressure increases, the films are deposited from a progressively more confined ablation plume. This might selectively affect both the energy and the efficiency of the single-species transferring to the growing film. This is what is likely happening also in the case of Bi_2Se_3 deposition, where heavy (i.e. Bi) and light (i.e. Se) elements can be stopped at different target-to-substrate distances, therefore determining slight changes in the Bi:Se chemical ratio (e.g. samples deposited at distance of 50 mm are slightly Se deficient).

XRD symmetrical $\theta-2\theta$ scans of optimized Bi_2Se_3 thin films only contain (001) peaks, indicating the preferential c -axis orientation of the film along the [001] Al_2O_3 and the [111] SrTiO_3 substrates crystallographic directions (Fig.1). By symmetric (0015) Bragg reflections, the out-of-plane c -axis parameters were found to be 2.861 nm and 2.862 nm for film grown on Al_2O_3 and SrTiO_3 substrates, respectively, thus indicating a substantial structurally relaxed growth on those substrates. Azimuthal ϕ -scan of Bi_2Se_3 thin films grown on Al_2O_3 (panel a of Fig.2) shows a substantial three-fold symmetry of the film which epitaxially grows on C-sapphire with a 60° in-plane rotation of the unit cell with respect to the substrate. The very low intensity of the second series of diffraction peaks at 60° from the major peaks indicates that the double-domain structure is strongly suppressed. However, even though showing the same c -axis preferential orientation, Bi_2Se_3 thin films grown on (111) SrTiO_3 substrate were not well ordered in the surface plane. In the azimuthal ϕ -scan (panel b of Fig.2), the second series of diffraction peaks is more intense than that reported for the film grown on (001) Al_2O_3 and the background signal is not-zero, thus indicating a fraction of in-plane randomly oriented Bi_2Se_3 domains.

Since XRD is a bulk sensitive technique, the surface order of the PLD grown films was also checked by LEED. In full agreement with the bulk sensitive XRD analyses, LEED pattern of in-situ transferred Bi_2Se_3 thin films grown on Al_2O_3 (panel c) of Fig.2) shows sharp diffraction spots exhibiting the expected three-fold symmetry,

thus confirming the Bi_2Se_3 triangular in-plane symmetry. However, films grown on the SrTiO_3 (panel d) of Fig.2) show broad diffraction spots exhibiting a six-fold symmetry with a continuous connecting ring indicating the presence of a randomly in-plane distributed disordered phase. In the case of Bi_2Se_3 thin films grown on SrTiO_3 substrates, the surface structural/electronics properties can be very unsuitable for device applications and/or advanced probing techniques (e.g. spin-resolved ARPES experiments on mis-oriented grains lead to very broad spectral features or even no detectable band dispersion). On the contrary, Bi_2Se_3 thin films grown on (001) Al_2O_3 show an almost unique in-plane structural arrangement thus making them ideal candidate in the cited cases.

The electronic properties and the chemical composition of Bi_2Se_3 thin films were explored by measuring core level photoemission spectra. The XPS survey scan displays main peaks of both Bi and Se²¹⁻²³ with no trace of either Bi²⁴ or Se²⁵ segregation. In case of pure Bi clusters, the 4f final states would show at 162.3 eV/157.0 eV binding energy (panel a) of Fig.3); for Se aggregates the binding would be at 55.1/55.3 eV with 0.86 eV spin-orbit splitting, well separated with respect to the observed peaks belonging to Bi_2Se_3 (panel b) in Fig.3). Details of the relevant core level peaks are presented in the panels of Fig.3, with the results of fitting routines to elucidate the lineshapes and energy separation. In panel a), the Bi 4f-Se 3p core lines show Se-related peaks shifting by 2.5 eV towards lower binding energies while Bi-peaks to higher binding energies (i.e. $\Delta E = 0.7$ eV), with respect to pure elemental aggregates. Such a behavior, attributed to the net charge flow with hybridized bonds between Bi and Se, is also observed on other Bi chalcogenide systems¹³.

Because of the large (i.e. 10%) experimental indetermination of the chemical composition from present XPS data due to possible errors in the fitting routine and background subtraction and the presence of photoelectron diffraction effects, as already reported in crystalline topological insulators^{26,27}, we performed energy dispersive spectroscopy (EDS) analysis, which is capable of an improved resolution in determining the chemical compo-

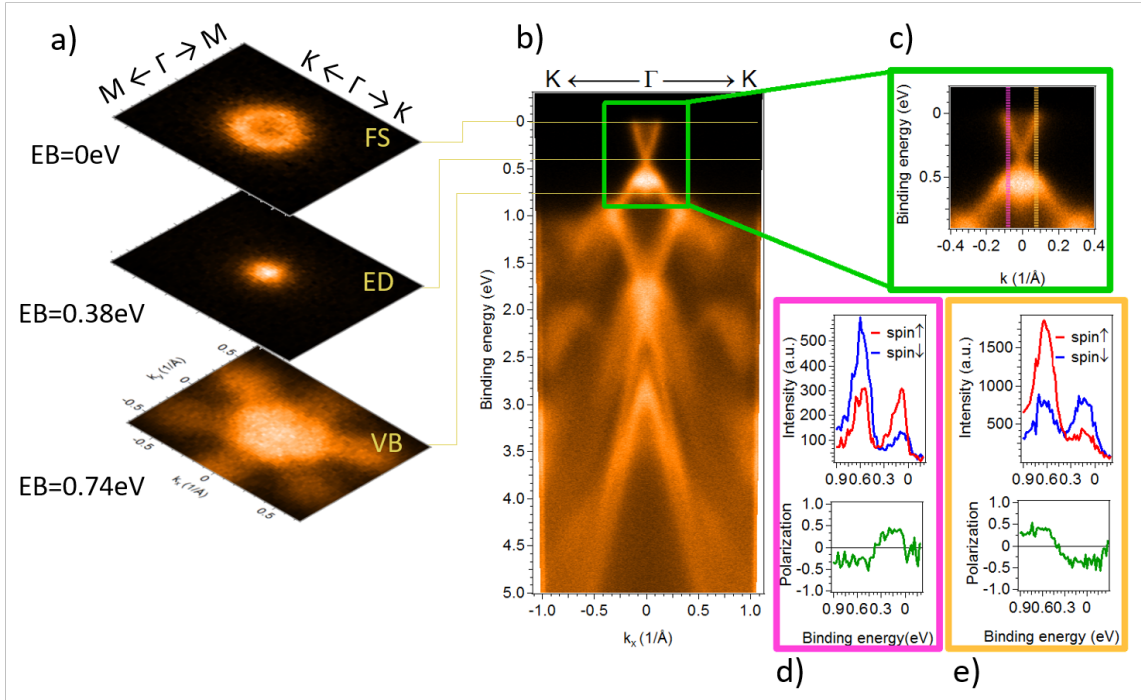


Figure 4. Spin-ARPES data of the topological surface state of a Bi_2Se_3 thin film: a) Constant energy contours at 0 eV (E_F), 0.38 eV (E_D) and 0.74 eV, respectively; b) valence band along the K- Γ -K high symmetry axis (photon energy is $h\nu = 55$ eV); c) zooming out of the topological surface state; d-e) spin-resolved curves and the corresponding spin polarization showing the spin texture of the Dirac cone extracted at $k_{||} = \pm 0.08 \text{\AA}^{-1}$.

sition (i.e. experimental error of about 5%). The Bi:Se chemical ratio was found to be 1.5, thus indicating a correct stoichiometry of the Bi_2Se_3 thin films. Interestingly, even in case of a slight Se-deficiency (for instance tuned by varying the target-to-substrate distance, as previously discussed), the topological properties (i.e. a single Dirac cone with well-defined spin-texturing) are not lost, while the Dirac cone is rigidly shifted to higher binding energies as already reported for thin films^{4,6} and also for single crystals^{29,30}.

Spin and angular resolved photoemission experiments were performed on in-situ transferred as-grown Bi_2Se_3 thin films at a temperature of 77 K and with a synchrotron radiation spot of about $100 \times 50 \mu\text{m}$. In order to better resolve the topological surface states features, ARPES investigation was performed at a suitable photon energy ($h\nu = 55$ eV) that strongly reduces the photoemission intensity from the bulk conduction band. ARPES data of a Bi_2Se_3 thin film grown on Al_2O_3 are shown in Fig.4.

The ARPES features (panels a), b) and c) of Fig.4) are well in agreement with the ones measured on cleaved single crystals²⁸ and thin films grown by MBE⁷. As a matter of fact, the characteristic signature of the topological surface state can be easily observed: two linearly dispersing metallic states cross the Fermi level at $k_{||} \sim \pm 0.1 \text{\AA}^{-1}$ and the two branches intersecting at Γ . The position of the Dirac point were determined by looking at the width of

several Momentum Distribution Curves (MDCs) of the ARPES spectrum and comparing the FWHMs. Dirac point was estimated to be at $E_B = 0.38 \pm 0.03$ eV binding energy, which is slightly larger than the expected value of 300 meV obtained by calculations³. It is worth noticing that such a discrepancy frequently occurs in Bi_2Se_3 thin films^{13,14} and also in single crystals^{2,7,31}. Such a result indicates the slight presence of Se vacancies, probably near the surface, which act as electron donor sites in the Bi_2Se_3 compound, populating the conduction band and shifting rigidly the band structure towards higher binding energies (e.g. for a Se:Bi ratio of about 1.38, Dirac point has been measured at about 0.6 eV). However, charge carrier density can be tuned by partially replacing Bi atoms with a very small amount ($\sim 0.6\%$) of divalent ions (e.g. Ca^{2+}) and thus having the bulk insulating behavior restored³¹.

The spin texture of the Dirac cone was mapped by using a very-low energy electron diffraction (VLEED) based vectorial spin polarimeter recently developed at APE-NFFA beamline³². Spin-resolved results, obtained along the quantization axis laying in the sample surface plane perpendicular to the crystalline momentum, are reported in panels d) and e) of Fig.4, where the spin-resolved curves and the spin polarization deduced from the Energy Distribution Curves (EDCs) measured at $k_{||} = \pm 0.08 \text{\AA}^{-1}$ in the k-space are shown. In particular, data confirm the expected helical spin texture of the topological in-

sulators: namely, two linear branches of the Dirac cone spin polarized characterized by opposite spin polarization for positive and negative momenta. Furthermore, as expected, the spin chirality reverses above and below the Dirac point. From the spin polarization analysis, the estimated polarization value is $\sim \pm 40\%$, lower than the expected 100%. However, such a feature is quite common, even in the case of single crystals, and it has been discussed thoroughly both from the theoretical as well as experimental point of view^{33–35}. Nevertheless, from the whole set of both ARPES and spin-ARPES results, it can be concluded that the PLD-grown Bi₂Se₃ thin films do show metallic surface states that evidence the spin features fingerprints of the topological insulators.

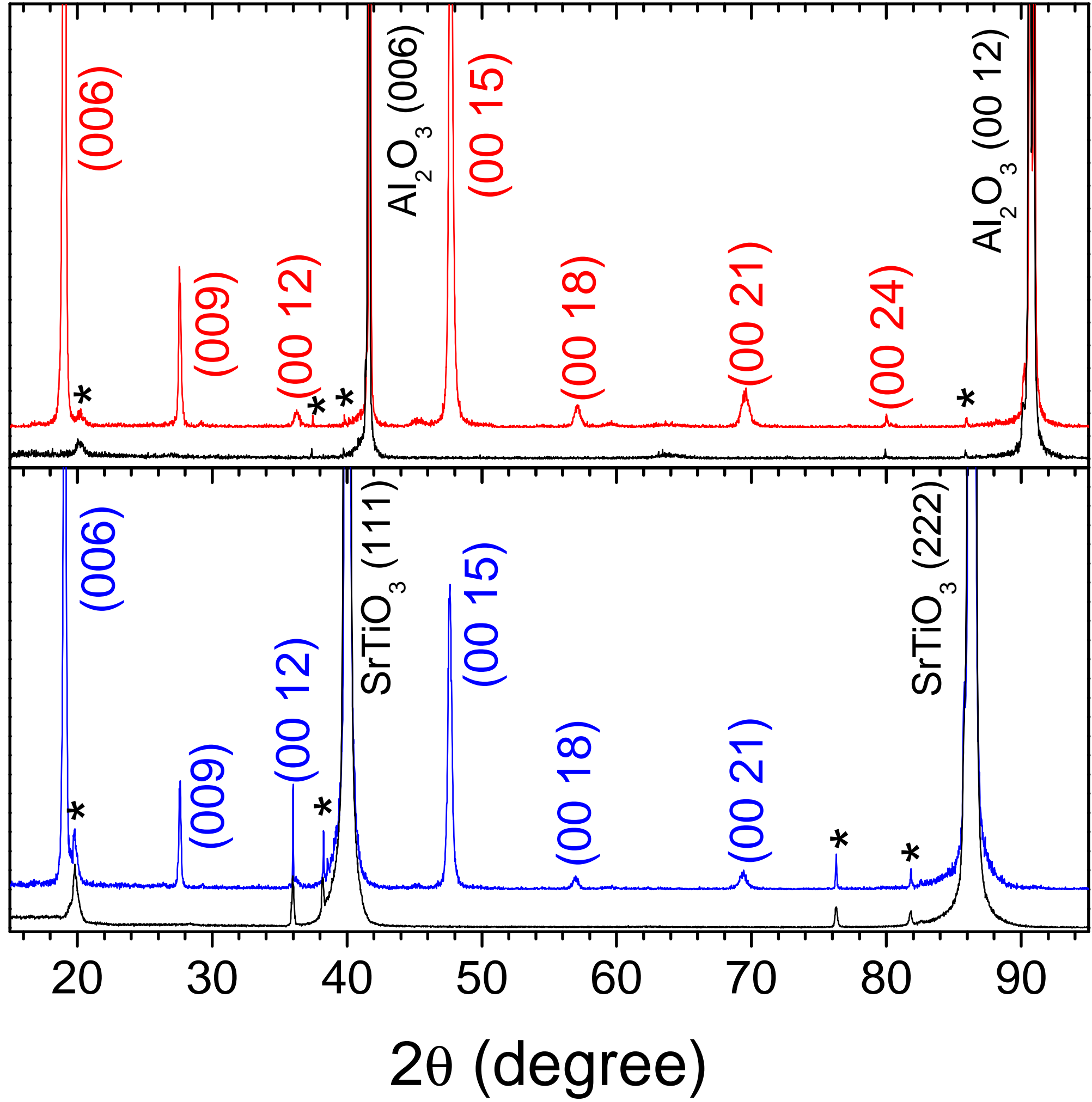
In conclusion, we have shown that high quality epitaxial Bi₂Se₃ thin films can be grown by Pulsed Laser Deposition. The combination of low deposition temperature (i.e. 290 °C), high deposition pressure (i.e. 0.1 mbar) and low deposition rate (i.e. 1 Hz) is crucial to obtain well ordered Bi₂Se₃ epitaxial thin films. Moreover, the use of (001) Al₂O₃ substrate provides an almost-unique structural texturing of the Bi₂Se₃ thin films. Spin-resolved ARPES data exhibit a single Dirac cone with a well-defined spin polarization texture of the topological surface states. Moreover, even in presence of a slight Se deficiency the topological surface states are protected and the Dirac cone is rigidly shifted towards higher binding energies. Such a feature opens perspectives in emerging spintronics planar devices based on multi-layered heterostructures technology in which one functional layer is the topological insulator Bi₂Se₃.

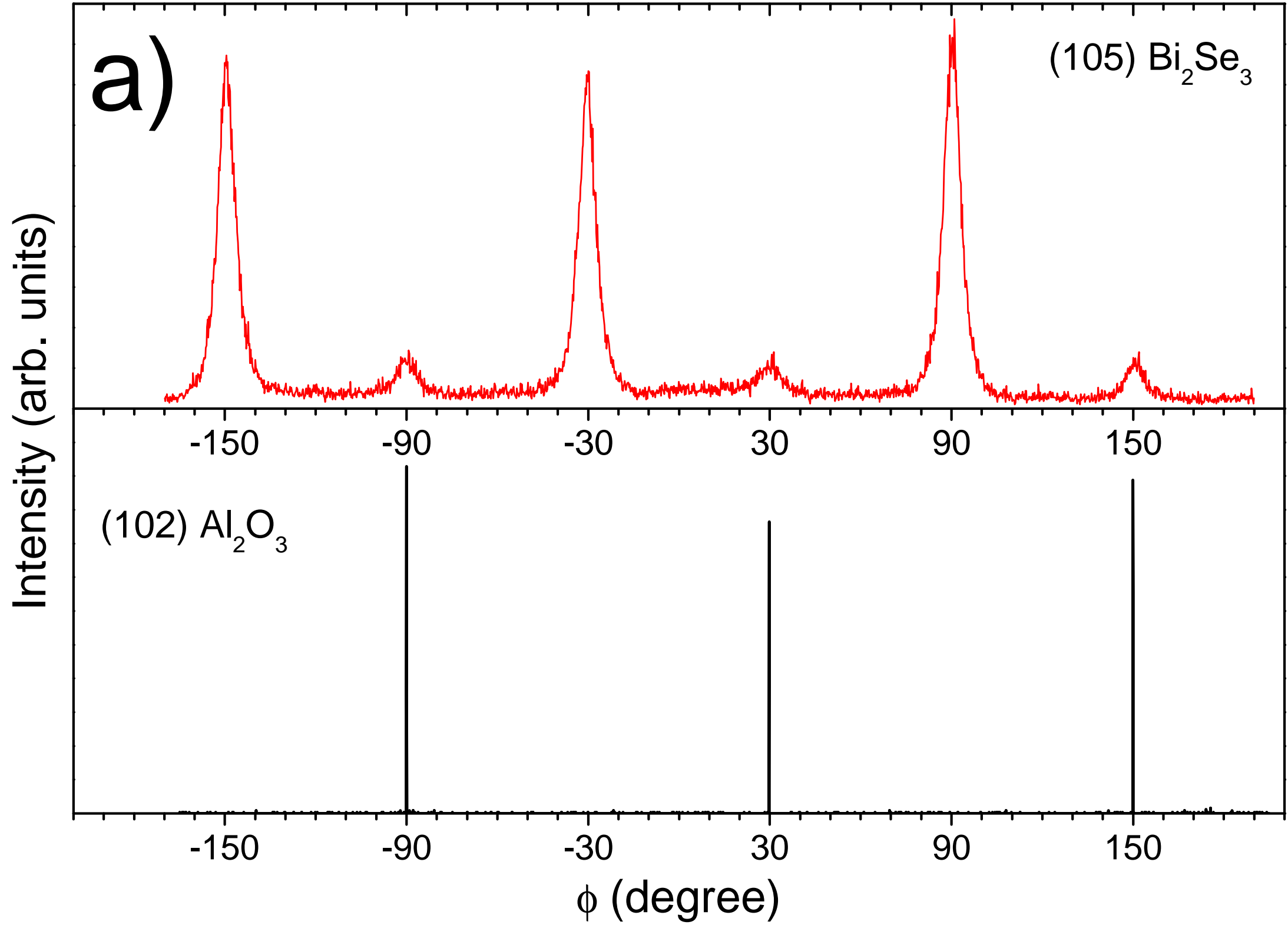
This work has been performed in the framework of the Nanoscience Foundry and Fine Analysis (NFFA-MIUR Italy Progetti Internazionali) facility. This work has been supported by NOXSS PRIN (2012Z3N9R9) Project of MIUR, Italy.

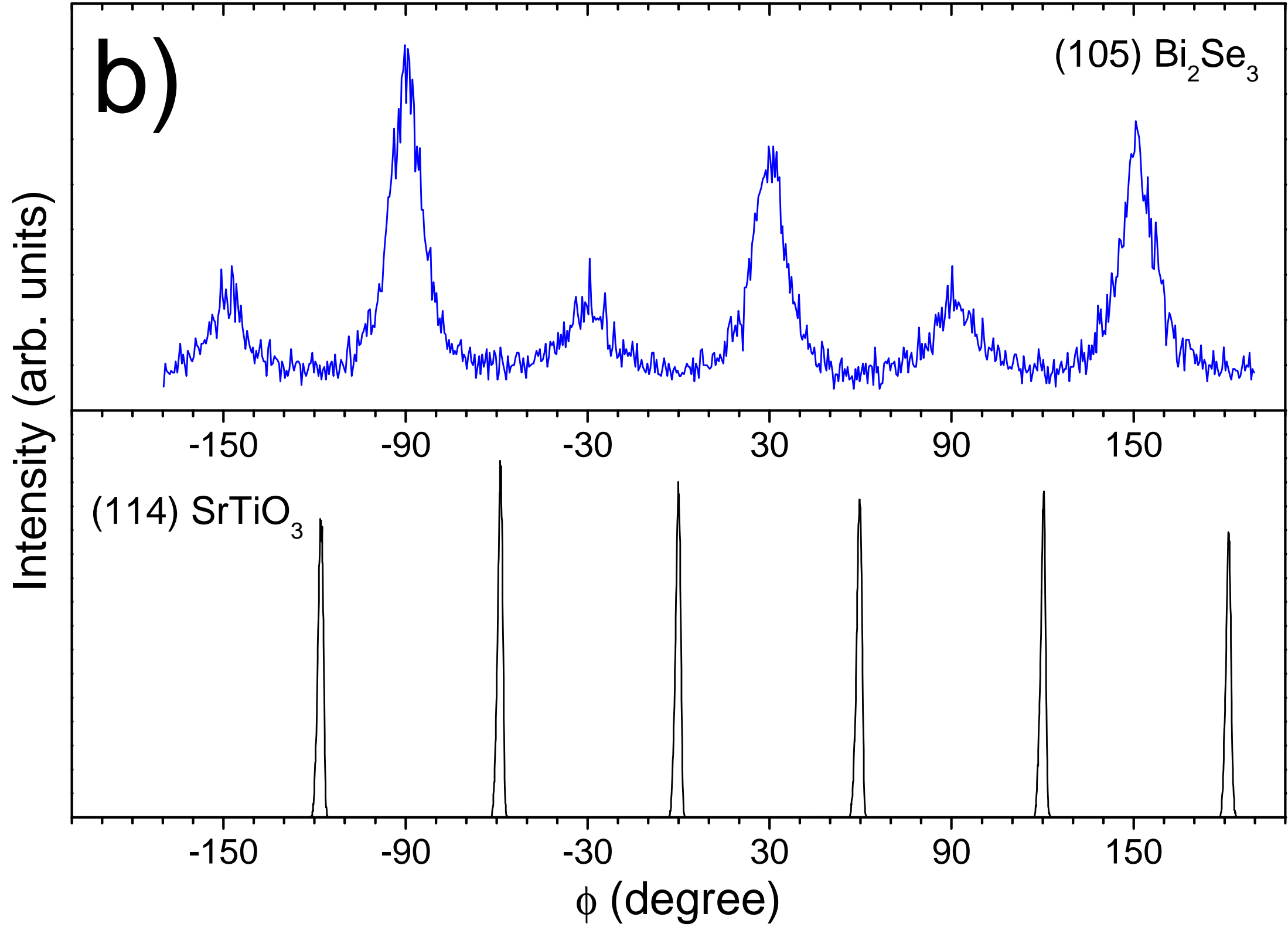
REFERENCES

- ¹L.Fu, C.L.Kane and E.J.Mele, Phys. Rev. Lett. 98, 106803 (2007).
- ²Y.Xia, D.Qian, D.Hsieh, L.Wray, A.Pal, H.Lin, A.Bansil, D.Grauer, Y.S.Hor, R.J.Cava and M.Z.Hasan, Nature Physics 5, 398 (2009).
- ³H.Zhang, C.-X. Liu, X.-L.Qi, X.Dai, Z.Fang and S.-C. Zhang, Nature Physics 5, 438 (2009).
- ⁴S.-Y.Xu, M.Neupane, C.Liu, D.Zhang, A.Richardella, L.A.Wray, N.Alidoust, M.Leandersson, T.Balasubramanian, J.Sanchez-Barriga, O.Rader, G.Landolt, B.Slonski, J.H.Dil, J.Osterwalder, T.-R.Chang, H.-T.Jeng, H.Lin, A.Bansil, N.Samarth and M.Z.Hasan, Nature Physics 8, 616 (2012).
- ⁵D.Zhang, A.Richardella, D.W.Rench, S.-Y.Xu, A.Kandala, T.C.Flanagan, H.Beidenkopf, A.L.Yeats, B.B.Buckley, P.V.Klimov, D.D.Awschalom, A.Yazdani, P.Schiffer, M.Z.Hasan, N.Samarth, Phys. Rev. B 86, 205127 (2012).
- ⁶H.M. do Nascimento Vasconcelos, M.Eddrief, Y.Zheng, D.Demaille, S.Hidki, E.Fonda, A.Novikova, J.Fujii, P.Torelli, B. Rache Salles, I.Vobornik, G.Panaccione, A.J.Aparecido de Oliveira, M.Marangolo, F.Vidal, ACS Nano 10, 1132 (2016).
- ⁷F.Vidal, M.Eddrief, B. Rache Salles, I.Vobornik, E.Velez-Fort, G.Panaccione, M.Marangolo, Phys. Rev. B 88, 241410(R) (2013).
- ⁸R.Mellnik, J.S.Lee, A.Richardella, J.L.Grab, P.J.Mintun, M.H.Fischer, A.Vaezi, A.Manchon, E.-A.Kim, N.Samarth and D.C.Ralph, Nature 511, 449 (2014).
- ⁹Y.Kubota, K.Murata, J.Miyawaki, K.Ozawa, M.C.Onbasli, T.Shirasawa, B.Feng, Sh.Yamamoto, R.-Y.Liu, S.Yamamoto, S.K.Mahatha, P.Sheverdyaeva, P.Moras, C.A.Ross, S.Suga, Y.Harada, K.L.Wang, I.Matsuda, arXiv:1604.04869 [cond-mat.mes-hall].
- ¹⁰<http://www.trieste.nffa.eu>
- ¹¹H.Lind, S.Lidin, and U.Haussermann, Phys. Rev. B 72, 184101 (2005).
- ¹²H.Okamoto, J. Phase Equilibria 15, 195 (1994).
- ¹³Y.F.Lee, S.Punugupati, F.Wu, Z.Jin, J.Narayan and J.Schwartz, Curr. Opin. Solid State Mater. Sci. 18, 279 (2014).
- ¹⁴P.H.Le, K.H.Wu, C.W.Luo, J.Leu, Thin Solid Films 534, 659 (2013).
- ¹⁵L.Meng, H.Meng, W.Gong, W.Liu, Z.Zhang, Thin Solid Films 519, 7627 (2011).
- ¹⁶G.Zhang, H.Qin, J.Teng, J.Guo, Q.Guo, X.Dai, Z.Fang, K.Wu, Appl. Phys. Lett. 95, 053114 (2009).
- ¹⁷P.H.Le, C.-N.Liao, C.W.Luo, J.-Y.Lin, J.Leu, Applied Surface Science 285P, 657 (2013).
- ¹⁸S.Schreyeck, N.V.Tarakina, G.Karczewski, C.Schumacher, T.Borzenko, C.Brüne, H.Buhmann, C.Gould, K.Brunner, L.W.Molenkamp, Appl. Phys. Lett. 102, 041914 (2013).
- ¹⁹Y.F.Lee, R.Kumar, F.Hunte, J.Narayan and J.Schwartz, J. Appl. Phys. 118, 125309 (2015).
- ²⁰P.Orgiani, R.Ciancio, A.Galdi, S.Amoroso, L.Maritato, Appl. Phys. Lett. 96, 032501 (2010).
- ²¹J.A.Bearden and A.F.Burr, Rev. Mod. Phys. 39, 125 (1967).
- ²²M.Cardona and L.Ley, *Photoemission in Solids I: General Principles*, Springer-Verlag, Berlin, Germany, 1978.
- ²³J.C.Fuggle and N.Mårtensson, J.Electron Spectrosc. Relat. Phenom. 21, 275 (1980).
- ²⁴A.S.Hewitt, J.Wang, J.Boltersdorf, P.A.Maggard, D.B.Dougherty, J. Vac. Sci. Technol. B 32, 04E103 (2014).
- ²⁵Y.-C. Yeh, P.-H. Ho, C.-Y. Wen, G.-J. Shu, R. Sankar, F.-C. Chou, C.-W. Che, J. Phys. Chem. C 120, 3314 (2016).
- ²⁶K.Kuroda, M.Ye, E.F.Schwieger, M.Nurmamat, K.Shirai, M.Nakatake, S.Ueda, K.Miyamoto, T.Okuda, H.Namatame, M.Taniguchi, Y.Ueda, A.Kimura, Phys. Rev. B 88, 245308 (2013).
- ²⁷M.V.Kuznetsov, L.V.Yashina, J.Sanchez-Barriga, I.I.Ogorodnikov, A.S.Vorokh, A.A.Volykhov, R.J.Koch, V.S.Neudachina, M.E.Tamm, A.P.Sirotina, A.Yu.Varykhalov, G.Springholz, G.Bauer, J.D.Riley, O.Rader, Phys. Rev. B 91, 085402 (2015).
- ²⁸J.G.Analytis, J.-H.Chu, Y.Chen, F.Corredor, R.D.McDonald, Z.X.Shen, I.R.Fisher, Phys. Rev. B 81, 205407 (2010).
- ²⁹D.Hsieh, Y.Xia, D.Qian, L.Wray, J.H.Dil, F.Meier, J.Osterwalder, L.Patthey, J.G.Checkelsky, N.P.Ong, A.V.Fedorov, H.Lin, A.Bansil, D.Grauer, Y.S.Hor, R.J.Cava, M.Z.Hasan, Nature 460, 1101 (2009).
- ³⁰J.G.Analytis, J.-H.Chu, Y.Chen, F.Corredor, R.D.McDonald, Z.X.Shen, I.R.Fisher, Phys. Rev. B 81, 205407 (2010).
- ³¹Z.Wang, T.Lin, P.Wei, X.Liu, R.Dumas, K.Liu, J.Shi, Appl. Phys. Lett. 97, 042112 (2010).
- ³²C.Biggi, J.Fujii, I.Vobornik, P.K.Das, D.Benedetti, F.Salvador, G.Panaccione, G.Rossi, arXiv:1610.06922 [physics.ins-det]
- ³³O.V.Yazyev, J.E.Moore, S.G.Louie, Phys. Rev. Lett. 105, 266806 (2010).
- ³⁴Z.-H.Zhu, C.N.Veenstra, S.Zhdanovich, M.P.Schneider, T.Okuda, K.Miyamoto, S.-Y.Zhu, H.Namatame, M.Taniguchi, M.W.Haverkort, I.S.Elifimov, A.Damascelli, Phys. Rev. Lett. 112, 076802 (2014).
- ³⁵G.Landolt, S.Schreyeck, S.V.Eremeev, B.Slonski, S.Muff, J.Osterwalder, E.V.Chulkov, C.Gould, G.Karczewski, K.Brunner, H.Buhmann, L.W.Molenkamp, J.H.Dil, Phys. Rev. Lett. 112, 057601 (2014).

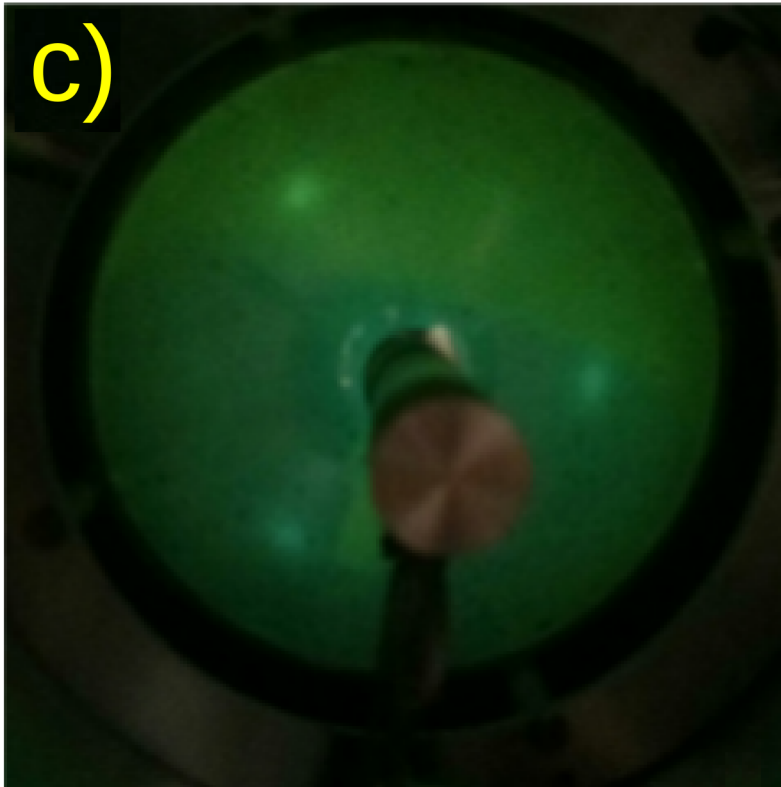
Intensity (arb. units)



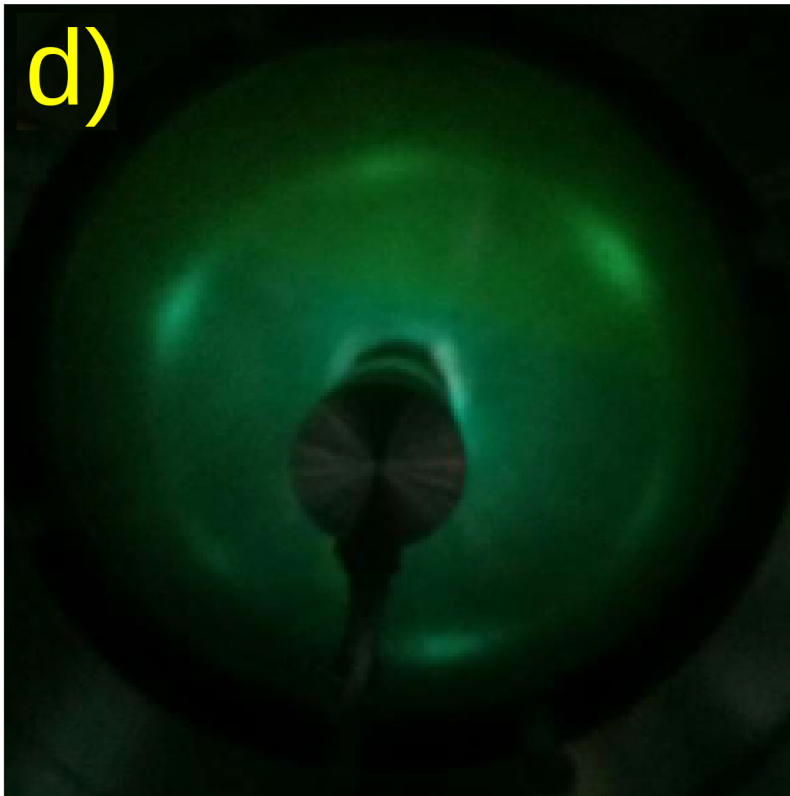


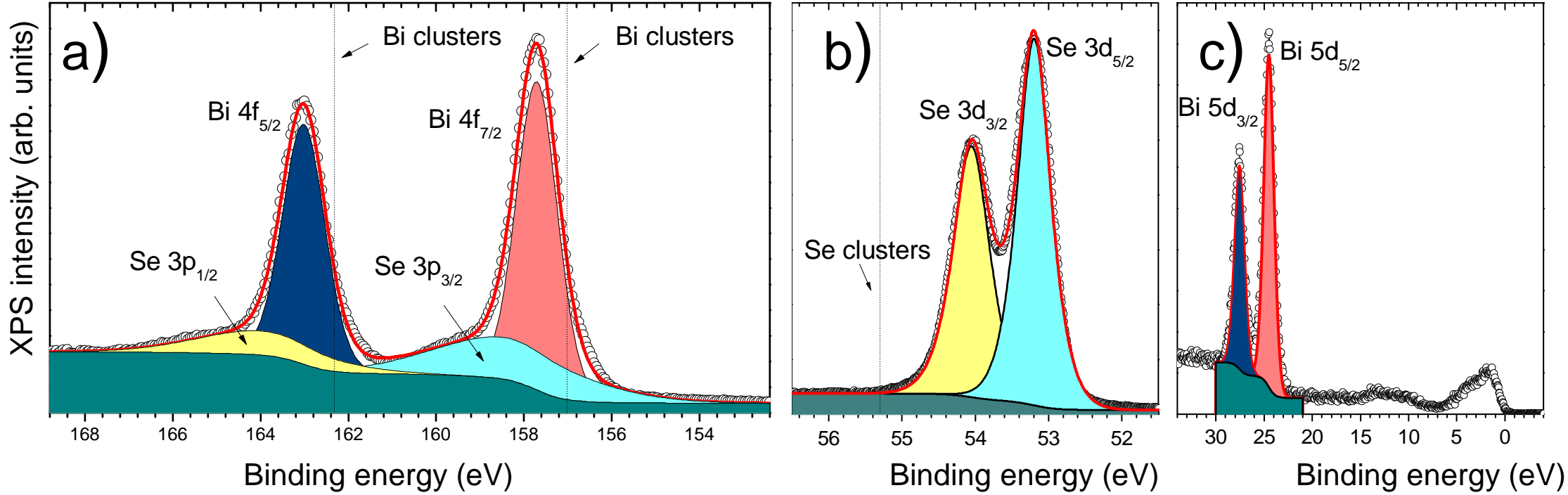


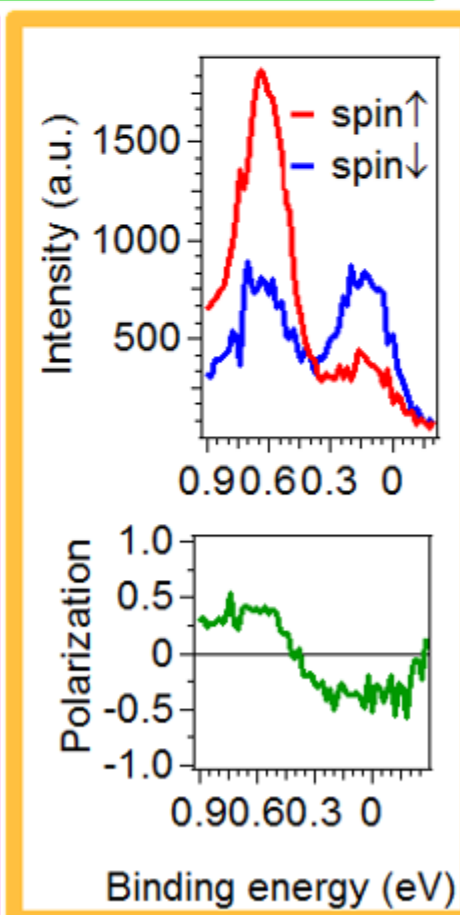
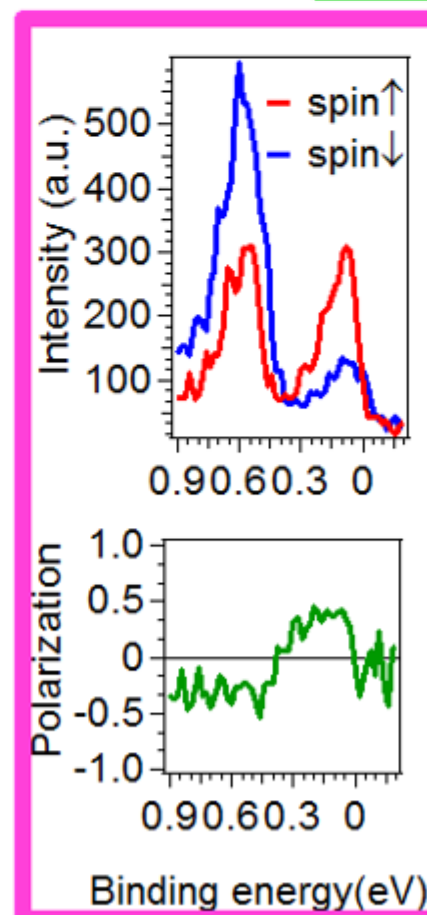
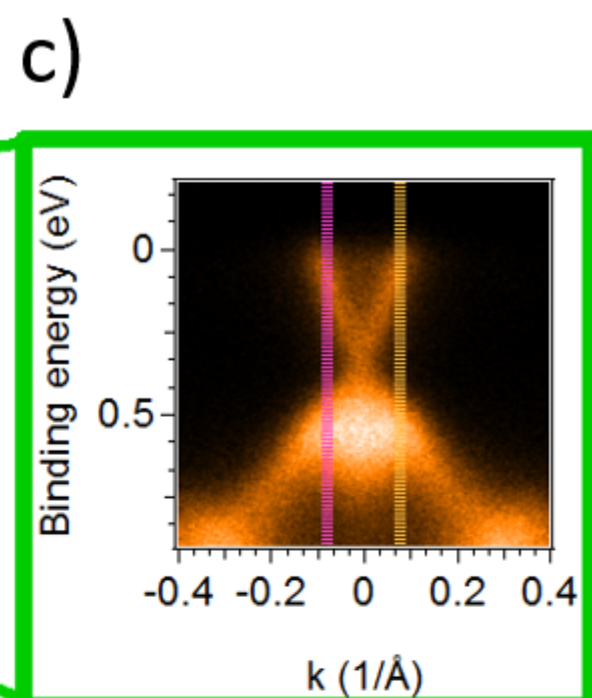
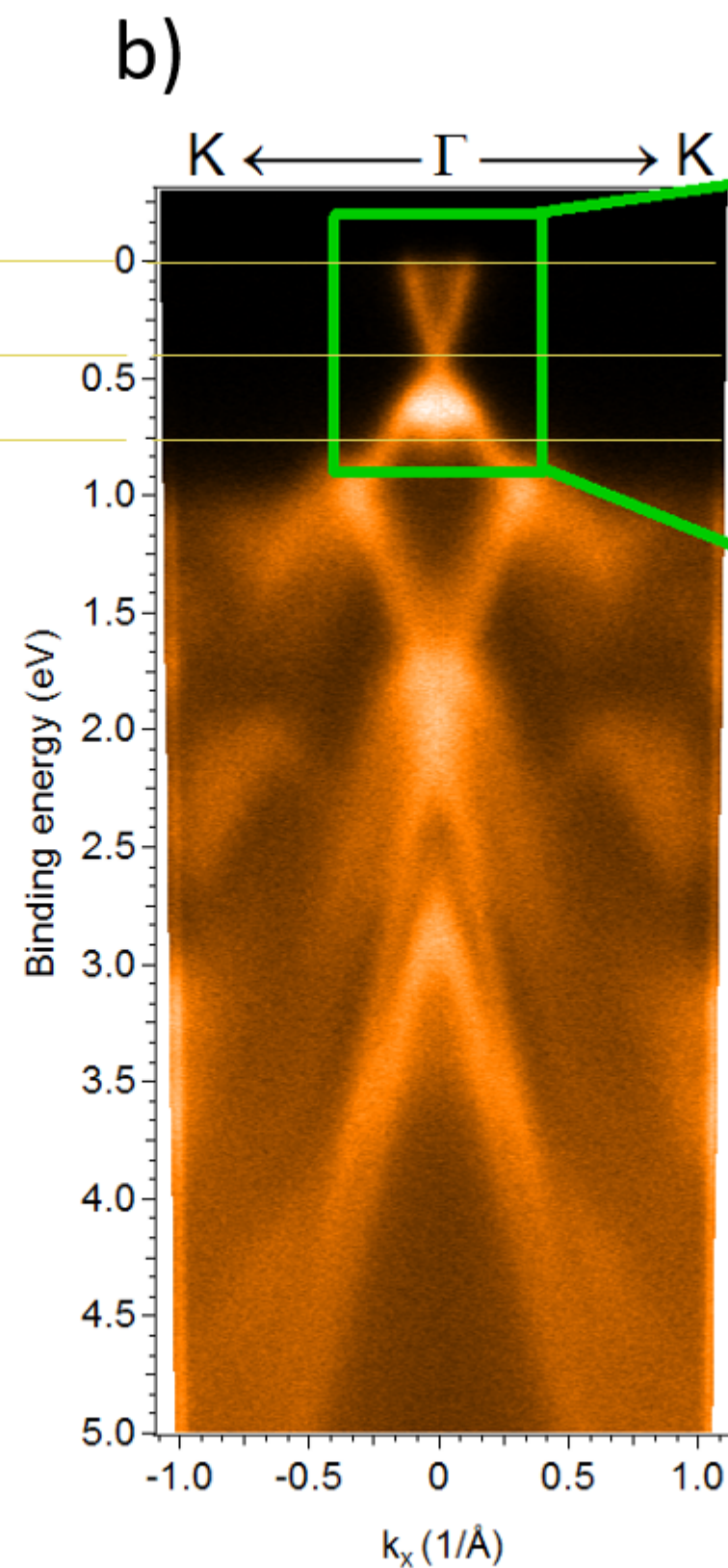
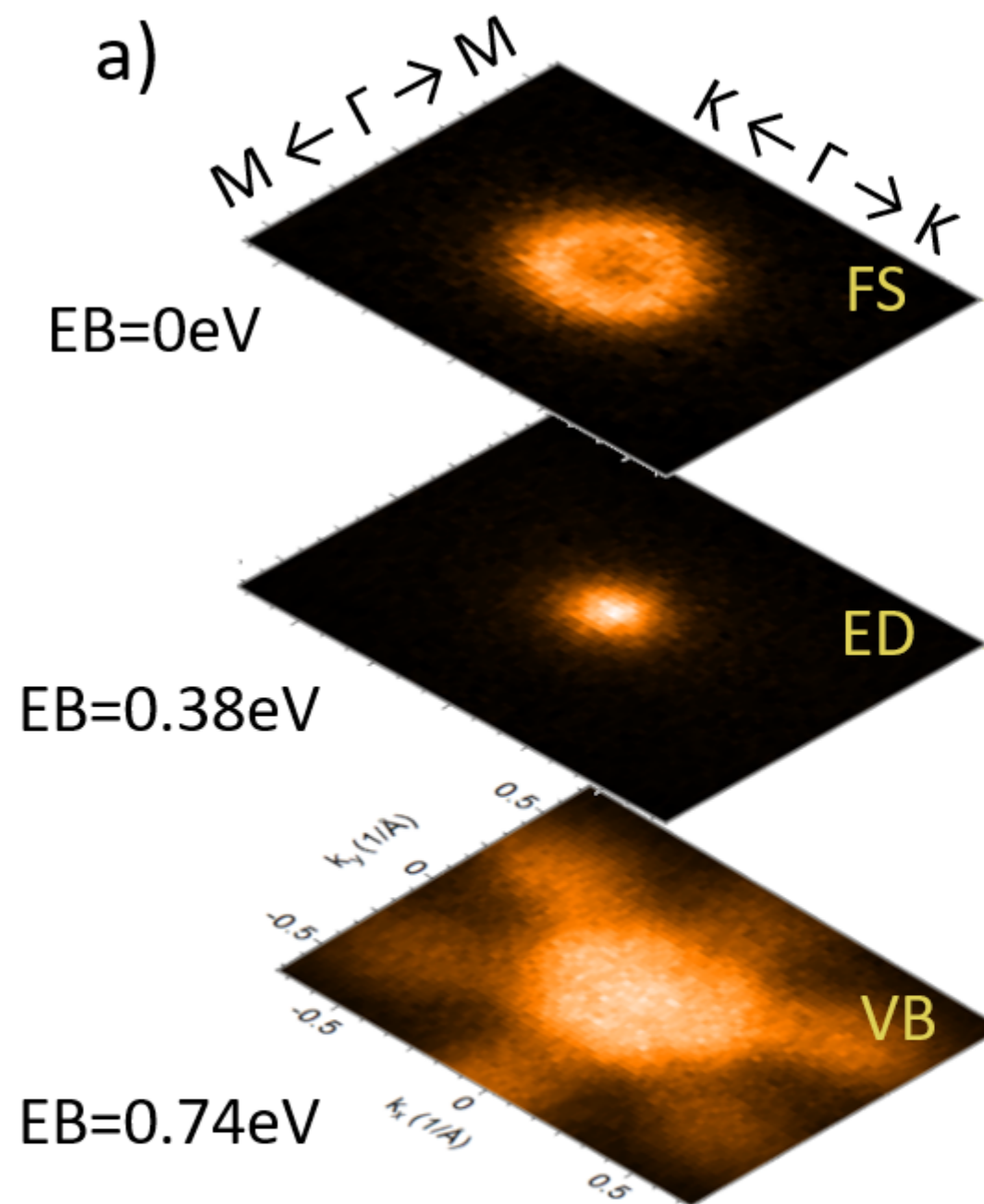
c)



d)







d)

e)